haematologica
Journal of the Ferrata Storti Foundation

Prognostic relevance of tumor-infiltrating CD4+ cells and total metabolic tumor volume-based risk stratification in diffuse large B-cell lymphoma

by Daisuke Ikeda, Mitsuaki Oura, Atsushi Uehara, Rikako Tabata, Kentaro Narita, Masami Takeuchi, Youichi Machida, and Kosei Matsue

Received: January 10, 2024.
Accepted: March 28, 2024.

Citation: Daisuke Ikeda, Mitsuaki Oura, Atsushi Uehara, Rikako Tabata, Kentaro Narita, Masami Takeuchi, Youichi Machida, and Kosei Matsue. Prognostic relevance of tumor-infiltrating CD4+ cells and total metabolic tumor volume-based risk stratification in diffuse large B-cell lymphoma. Haematologica. 2024 Apr 4. doi: 10.3324/haematol.2024.285038 [Epub ahead of print]

Prognostic relevance of tumor-infiltrating CD4$^+$ cells and total metabolic tumor volume-based risk stratification in diffuse large B-cell lymphoma

Daisuke Ikeda[1*], Mitsuaki Oura[1], Atsushi Uehara[1], Rikako Tabata[1], Kentaro Narita[1], Masami Takeuchi[1], Youichi Machida[2] and Kosei Matsue[1]

[1]Division of Hematology/Oncology, Department of Medicine, Kameda Medical Center, Chiba, Japan; [2]Department of Radiology, Kameda Medical Center, Chiba, Japan.

[*]**Correspondence:** Daisuke Ikeda, M.D., Division of Hematology/Oncology, Department of Medicine, Kameda Medical Center, 929 Higashi-chou, Kamogawa-shi, Chiba 296-8602, Japan
Tel.: +81-470-92-2211; Fax: +81-470-92-2211; e-mail: dskikd.2409@gmail.com

Running title: Tumor-infiltrating CD4+ cells and TMTV in DLBCL
Keywords: Tumor-infiltrating CD4+ cells, PET/CT, TMTV, DLBCL

Acknowledgment: We would like to Takashi Nazuka, Tomoe Ando, and Tsubasa Murata (Haematology section of Central Laboratory, Kameda Medical Center) for their excellent help in performing the flow cytometry analysis. We would also like to thank Dr. Hajime Senjo (Department of Haematology, Hokkaido University) and Dr. Kenji Hirata (Department of Nuclear Medicine, Hokkaido University) for assisting with the use of the Metavol software. We would also like to thank Editage (www.editage.jp) for providing excellent English language editing assistance.

Author Contribution: D.I. and K.M. designed the study, interpreted the data, performed the statistical analysis, provided patient care, and wrote the manuscript. Y.M. interpreted the imaging findings. M.O., A.U., R.T., K.N., and M.T. provided patient care. All authors critically reviewed and approved the manuscript.

Conflict of interest disclosure: KM received a research grant from AstraZeneca. Other authors declare no competing financial interests.

Data availability statement: The datasets generated and analysed in the current study are available from Daisuke Ikeda upon reasonable request.

Abstract

To elucidate the relationship between pre-treatment radiomic parameters and the proportions of various tumour-infiltrating (TI) cells, we retrospectively analysed the association of total metabolic tumour volume (TMTV) and TI cells on biopsied tumour lesions in 171 patients with newly diagnosed diffuse large B-cell lymphoma (DLBCL). The surface markers of TI cells were analysed by multicolour flow cytometry using a dissected single-cell suspension. In examining the correlation between TI cells and PET-derived parameters (SUV_{max}, TMTV, and total lesion glycolysis), intratumoural cell types minimally influenced the results, except for a weak negative correlation between CD4+ cells and SUV_{max} (R=-0.16, P=0.045). Even for the lesion fluorodeoxyglucose uptake at the biopsied site, CD19+ cells (indicative of malignant burden) showed only a weak correlation with the highest SUV (R=0.21, P=0.009), whereas CD3+ (R=-0.25, P=0.002) and CD4+ cells (R=-0.29, P<0.001) demonstrated a similarly weak inverse correlation. High TMTV and low TI CD4+ cells were independently associated with poor prognosis and their combination identified the most adverse population (3-year progression-free survival: 32.3%, 95% confidence interval [CI]: 19.4%-53.7%; 3-year overall survival: 48.4%, 95% CI: 33.6%-69.6%). Moreover, radiomic parameters incorporating the international prognostic index significantly improved the 3-year survival prediction (area under the curve: 0.76, P<0.05) compared to their standalone use. This study underscores the prognostic impact of TI CD4+ cells on DLBCL and suggests that integration of TMTV and TI cell analysis enhances the accuracy of prognostic prediction.

Introduction

Diffuse large B-cell lymphoma (DLBCL) is a predominantly aggressive non-Hodgkin lymphoma (NHL) affecting adults.[1] DLBCL is biologically heterogeneous,[2] exhibiting variable responses to curative-intent chemotherapy. Approximately one-third of patients relapse after first-line treatment,[1] leading to dismal outcomes despite advances in salvage therapeutic strategies, including chimeric antigen receptor (CAR) T-cell therapies and bispecific antibodies.[3, 4] In light of these challenges, there is an urgent need to develop more sophisticated risk stratification models at diagnosis beyond the conventionally adopted International Prognostic Index (IPI)-based system.[5-7] Despite recent progress in understanding the genomic landscape,[8] the implementation of molecular profiling into clinical practice, such as double-hit signatures[9, 10] and genetic clustering,[2, 11] has been limited to a few advanced facilities.

Fluorine-18 fluorodeoxyglucose-positron emission tomography/computed tomography (^{18}FDG-PET/CT) is recommended as part of the diagnostic work-up for precise staging.[12] Notably, multiple functional radiomic features can be extracted from PET/CT. Total metabolic tumour volume (TMTV) represents the estimated tumour burden, while total lesion glycolysis (TLG) considers both tumour volume and metabolic activity. Recently, metabolic heterogeneity, denoting intratumour heterogenous ^{18}FDG uptake, has been reported to have prognostic value in DLBCL[13, 14] and different solid tumours.[15] Among these parameters, TMTV stands out as the most extensively validated for its prognostic utility in various study settings.[16] Notably, due to its ease of acquisition from PET/CT, minimal interobserver variation, and high reproducibility with full or semi-automated segmentation software,[17] TMTV has been accepted as a biomarker, either on its own[18, 19] or in combination with other indicators.[20-23]

However, PET/CT cannot differentiate between the ^{18}FDG uptake of different intratumoural cellular components and genuine tumour uptake. Consequently, TMTV may not accurately represent the actual tumour burden of malignant B-cells. Moreover, numerous studies have characterized the DLBCL tumour milieu at the cellular level,[24-28] showing that an enrichment of tumour-infiltrating (TI) T-cells is associated with a more favourable prognosis.[29-33]. Although TI T-cells may reflect the FDG-uptake at the baseline PET/CT, their role as a pre-treatment PET/CT parameter in DLBCL remains undefined. To date, there is no data on the simultaneous quantification of tumour volume and cell content in DLBCL. Thus, this study aimed to elucidate the association between lymphocytes infiltrating the tumour tissue, including their subset, and TMTV measured by PET/CT in DLBCL. We anticipate that elucidation of this association could potentially refine the current risk stratification of patients with DLBCL by PET/CT and IPI.

Methods

Patient cohort and study design

We conducted a retrospective analysis of newly diagnosed patients with histologically confirmed DLBCL who were treated with rituximab combined with cyclophosphamide, doxorubicin, vincristine, and prednisone (R-CHOP) or R-CHOP-like chemotherapy at Kameda Medical Center between 2006 and 2020. Primary exclusion criteria were based on availability, specifically the absence of pre-treatment PET/CT with ^{18}FDG-avid lesions and the insufficient

flow cytometric (FCM) data from biopsied lymphoma lesions. Patients with high-grade B-cell lymphoma harbouring concurrent rearrangements of MYC and BCL2 and/or BCL6 were also excluded. The present study was conducted in accordance with the Declaration of Helsinki and was approved by our institutional review board (approval number: 22-095).

Measurement of PET/CT-derived parameters

All PET/CT images were acquired according to our institution's standardized protocol.[34] TMTV was defined as the sum of the volume of visually identified lymphoma lesions with a standardized uptake value (SUV) of ≥ 4.0 as the absolute threshold. TLG was calculated by multiplying TMTV by the mean SUV. For tumour delineation and calculation of these radiomic features, a semi-automatic computer-aided analysis of PET/CT images was performed using the open-source software Metavol (Hokkaido University, Sapporo, Japan). Considering the spatial heterogeneity, the lesion PET/CT parameters obtained from biopsied sites were also measured (Figure 1A).

Quantification of intratumoural cell populations

Briefly, sampled lymph nodes (LN) or extranodal (EN) lesions were mechanically dissociated into cell suspensions, then washed, incubated, and stained with a panel of antibodies including CD45-KrO, CD19-APC, CD3-FITC, CD4-FITC, CD8-PE, and CD56-PE (if available). Proportions of CD19+, CD3+, CD4+, CD8+, and CD56+ cells within the acquired monoclonal cells were quantified after gating based on the characteristic forward and side scatter patterns and CD45 positivity specific to lymphocytes (Figure 1B). While the tissue sampling manner was not strictly limited to an excisional biopsy, a minimum of 10000 mononuclear cells per sample was required, based on a previous study.[31] Data were acquired on a Navios flow cytometer using the Kaluza software (Beckman Coulter, CA, USA).

Statistical analysis

Statistical analyses were performed with R version 4.1.1 (R Foundation, Vienna, Austria). Pearson correlation analysis was employed to examine the relationships between radiomic features and cellular content within tumours. To maximize predictive power, optimal cut-off values were determined using receiver operating characteristic (ROC) curves for 3-year progression-free survival (PFS) and 3-year overall survival (OS). The PFS and OS were estimated using the Kaplan–Meier methods and compared with the log-rank test. Univariate and multivariate analyses were conducted using Cox proportional hazards models to assess the factors affecting PFS and OS. Statistical significance was defined as a two-sided P-value of <0.05. Methods are further detailed in Supplementary materials.

Results

Overall patient characteristics

In total, 171 out of 518 patients were included in the analysis (Supplementary Figure 1) based on the inclusion and exclusion criteria. Regarding subtypes, 156 (91.2%) were DLBCL-not otherwise specified, eight (4.7%) were DLBCL histologically transformed from follicular lymphoma, and seven (4.1%) were Epstein-Barr virus

(EBV)-positive DLBCL. The median age was 71 years (interquartile range [IQR]: 61-79). Approximately half of the patients (48.0%) were categorized as IPI 3-5. Using the Hans algorithm,[35] cell of origin (COO) was determined in 137 patients (80.1%), 48 (35.0%) of whom were GCB type and 89 (65.0%) were non-GCB type. This higher proportions of non-GCB type may reflect the geographical distribution of activated B-cell-like DLBCL in Asian countries.[36,37]

Most patients (87.1%) received R-CHOP, with a complete remission rate of 81.3% at the end of induction according to the Lugano 2014 criteria. During the median observation period of 51 months, 68 patients (39.8%) died and 81 (47.4%) experienced PFS events, resulting in the estimated median OS and PFS of 140 months (95% confidence interval [CI]: 96-not reach [NR]) and 81 months (95% CI: 38-NR), respectively.

Correlation between tumour-infiltrating cells and PET-derived parameters

One hundred forty-four patients (84.2%) were biopsied at a LN while the remaining 27 (15.8%) were biopsied at an EN lesion. The biopsy sites matched the lesions with SUV_{max} in 89 (52.0%) patients. The median percentage of CD19+, CD3+, CD4+, CD8+ and CD56+ cells (n=120) in the biopsied lesion were 41.5% (IQR: 20.5-60.3), 49.8% (IQR: 29.5-67.6), 26.3% (IQR: 13.8-42.7), 16.2% (IQR: 9.5-23.1) and 0.6% (IQR: 0.4-1.2), respectively.

The median SUV_{max}, TMTV, and TLG were 20.8 (IQR: 14.9-26.8), 177.8 mL (IQR: 47-560), and 1683 (IQR: 351.9-5557.4), respectively. The correlation between quantified cellular components in biopsied lesions and functional PET-derived parameters is shown in Figure 2. Intriguingly, SUV_{max}, TMTV, and TLG were not significantly influenced by intratumoural cell types except for a weak negative correlation between CD4+ cells and SUV_{max} (R=-0.16, P=0.045) (Figure 2A-C). Even for the lesion ^{18}FDG uptake, CD19+ cells indicative of the malignant cell burden exhibited only a weak correlation with the highest SUV (SUV_{lesion}) and SUV_{mean} within the biopsied site (R=0.21, P=0.009), while CD3+ and CD4+ cells exhibited a correspondingly inverse weak correlation (CD3+ R=-0.25, P=0.002 and CD4+ R=-0.29, P<0.001) (Figure 2D). Neither the overall nor the lesion radiomic parameters were correlated with CD8+ cell proportions.

Determination of optimal cut-off values

ROC analysis for determining the optimal cut-off of TI-cell populations and radiomic features is displayed in Supplementary Figure 2. CD4+ T-cells had the highest area under the curve (AUC) for both 3-year PFS (AUC: 0.61; specificity [Sp]: 0.69, sensitivity [Se]: 0.48) and OS (AUC: 0.62; Sp 0.6, Se 0.61), with corresponding cut-off values of 22.1% and 24.6%, respectively. For simplicity, CD4+ <24% was defined as low CD4+ cell infiltration for further analysis. In contrast, CD8+ and CD19+ cells demonstrated notably lower predictive value, with AUCs approaching 0.5.

Regarding PET/CT findings, TMTV and TLG exhibited nearly overlapping ROC curves, with TMTV having a slightly higher AUC (3-year PFS AUC: 0.64, Sp: 0.73, Se 0.55 for TMTV vs. AUC: 0.63, Sp: 0.64, Se: 0.57 for TLG; 3-year OS AUC: 0.62, Sp: 0.68, Se: 0.57 for TMTV vs. AUC: 0.61, Sp: 0.61, Se: 0.57 for TLG). The cut-off value of TMTV for predicting both 3-year PFS and OS was determined to be 314 mL. Using these thresholds, 76 (44.4%) patients with low TI-CD4+ cells and 66 (38.6%) patients with high TMTV were identified.

Survival outcomes according to intratumoural CD4+ cell levels and tumour burden

Patient characteristics according to TI-CD4+ cell proportions are shown in Table 1. Comparable values for TMTV, baseline IPI components, IPI category, and COO were observed between groups with high and low intratumoural

CD4+ cell burden, except for a lower prevalence of Eastern Cooperative Oncology Group performance status (ECOG PS) score≥2 with marginal significance (14.5% vs. 27.4%, P=0.065) in those with low intratumoural CD4+ cells. Reflecting the smaller number of patients with impaired PS, those with low TI-CD4+ cells were significantly more likely to receive standard R-CHOP or more intensive chemotherapy than those without (98.7% vs. 91.6%, P=0.044). Notably, none of the patients with EBV-positive DLBCL were classified in the low TI-CD4+ cell group. Compared to EBV-negative DLBCL, EBV-positive cases had significantly higher proportions of intratumoural CD3+ (median 81.2% vs. 66.8%, P=0.016) and CD8+ T-cells (median 22.9% vs. 15.8%, P=0.011), as well as a non-significant trend toward increased CD4+ cells (median 35.7% vs. 26.0%, P=0.093), which may represent the distinct immune-evasive properties of EBV-positive DLBCL (Supplementary Figure 3).[38]

Figure 3 shows the PFS and OS according to the levels of TI-CD4+ cells and TMTV. Despite the above-mentioned favorable clinical factors, which were biased towards patients with low TI-CD4+ cells, these individuals had significantly poorer PFS and OS compared to those with high TI-CD4+ cells (3-year PFS: 50.7%, 95% CI: 40.6%-63.4% vs. 64.4%, 95% CI: 55.3%-75.0%, P=0.025; 3-year OS: 64.0%, 95% CI: 54.0%-75.9% vs. 79.6%, 95% CI: 71.9%-86.2%, P=0.002). Even when restricted to the 27 patients with biopsy sites in EN lesions, significantly worse PFS and OS persisted (3-year PFS: 13.3%, 95% CI: 3.6%-48.4% vs. 54.5%, 95% CI: 31.8%-93.6%, P=0.006; 3-year OS: 53.3%, 95% CI: 33.2%-85.6% vs. 72.7%, 95% CI: 13.4%-50.6%, P=0.033) (Supplementary Figure 4). Similar to low TI-CD4+ cells, elevated TMTV also significantly worsened PFS (3-year PFS rate: 40.3%, 95% CI: 30.0%-54.2% vs. 69.8%, 95% CI: 61.4%-79.3%, P<0.001) and OS (3-year OS rate: 60.2%, 95% CI: 49.4%-73.4% vs. 80.5%, 95% CI: 73.2%-88.5%, P<0.001).

Intratumoural CD4+ cell levels influence the TMTV-based stratification

We also examined the prognostic impact of TI-CD4+ cells on TMTV-based outcome stratification (Figure 4). Patients with low TMTV and high TI-CD4+ cells showed markedly improved PFS (3-year PFS: 74.4%, 95% CI: 63.9%-86.5%) and OS (3-year OS: 84.7%, 95% CI: 75.9%-94.4%) compared to those with high TMTV and low TI-CD4+ cells. The latter group experienced unfavourable outcomes, with a 3-year PFS of 32.3% (95% CI: 19.4%-53.7%) and a 3-year OS of 48.4% (95% CI: 33.6%-69.6%). The prognostic relevance of TI-CD4+ cells was pronounced among high-TMTV cases, with significant outcome differences observed (P=0.033 and P=0.006 for PFS and OS, respectively).

On univariate analysis, low TI-CD4+ cells, high TMTV, and IPI 3-5 were significantly associated with worse PFS (low TI-CD4+ cells hazard ratio [HR]: 1.64, 95% CI: 1.05–2.54, P=0.027; high TMTV HR: 2.59, 95% CI: 1.67–4.02, P<0.001; IPI 3-5 HR: 2.64, 95% CI: 1.67–4.17, P <0.001) and OS (low TI-CD4+ cells HR: 2.09, 95% CI: 1.29–3.40, P=0.003; high TMTV HR: 2.56, 95% CI: 1.58–4.15, P<0.001; IPI 3-5 HR: 2.39, 95% CI: 1.46–3.92, P=0.001) (Table 2). All these variables retained a prognostic significance on multivariate analysis (all P <0.05 for PFS and OS), except for IPI 3-5 for OS (HR: 1.75, 95% CI: 0.96-3.21, P=0.068).

Integration of tumour volume and its content enhances risk prediction based on IPI

Based on the results of the multivariate analysis, we constructed a novel predictive model that included the variables TI-CD4+ cell level, TMTV level, and IPI category. The ROC curve showed that the combined use of these three indices as continuous variables significantly outperformed their individual use in predicting 3-year OS (combined model AUC: 0.76, Sp: 0.72, Se: 0.76; IPI only AUC: 0.7, Sp: 0.59, Se: 0.7; CD4+ cell proportion only AUC:

0.62, Sp: 0.6, Se: 0.62; TMTV only AUC: 0.61, Sp: 0.68, Se: 0.61, all P<0.05) (Figure 5A). Finally, patients were categorized into four groups based on the number of risk factors defined as IPI scores of 3-5, low levels of TI-CD4+ cells, and high TMTV (Figure 5B). Among 89 patients with IPI 0-2, approximately half had additional risk factors of either low TI CD4+ cells or high TMTV (n=39, 43.8%) or both low TI CD4+ cells and high TMT (n=7, 7.9%). Meanwhile, the resting 82 patients with IPI 3-5 were divided into those with one (n=17 [20.7%]), two (n=41 [50.0%], and three risk factors (n=24 [29.3%]). This stratification system almost equally discriminated the outcomes (Figure 5C-D). Patients without any risk factors had an excellent 3-year PFS of 85.6% (95% CI: 75.5%-97.0%) and OS of 92.9% (95% CI: 85.5%-100%). In contrast, patients with all three risk factors had the worst outcomes with a 3-year PFS of 33.3% (95% CI: 18.9%-58.7%) and OS of 50.0% (95% CI: 33.5%-74.6%).

Discussion

This study elucidated the relationship between pre-treatment radiomic parameters and the proportions of various tumour-infiltrating cells in DLBCL. Neither malignant B-cells nor other immune cells had a substantial impact on the maximum or average ^{18}FDG uptake and tumour volume, even within locally biopsied LNs. Among the non-malignant cellular components, CD4+ cells had the highest and independent prognostic value, better stratifying patients with a similar tumour burden status. Consequently, the combination of low TI-CD4+ cells and high TMTV improved the prognostic performance of the routinely used IPI system.

Over the two decades since the development of rituximab and IPI, outcomes and classification of patients with DLBCL have been improved but remains unsatisfactory. Recently, two large studies from clinical trials (the REMARC [n=1305] and GOYA [n=301] studies) highlighted TMTV as a robust prognosticator, with the determined cut-off values ranging from 220 mL (41% maximum SUV threshold method)[19] to 366 mL (a tumor threshold of 1.5 times the mean SUV of the liver +2 standard deviations).[18] The new international metabolic prognostic index integrates TMTV as a continuous variable with age and stage, enabling robust and personalized patient outcome predictions.[39] Earlier studies suggested that the high baseline tumour burden leads to reduced exposure to rituximab and contributed to poorer outcomes.[40, 41] Moreover, there has been growing interest in quantitative volumetric assessment with the discovery that high pretherapy TMTV is a major risk factor for early treatment failure of CAR T-cell therapies.[42, 43]

Despite the limitation that the ^{18}FDG tracer detects glucose uptake by all viable cells, potentially diminishing the prognostic utility of PET/CT, the influence of intratumoural components on metabolic activities and tumour burden is scarcely studied in NHL. As of writing, the only existing study pertains to follicular lymphoma, where the malignant B-cell burden within individual lymphoma lesions was the main determinant of TMTV, and tumour-infiltrating T-lymphocytes positively influenced SUV_{max}.[44] Intriguingly, our DLBCL cohort presented contrasting results: only intratumoural CD4+ cells weakly contributed to a lower SUV_{max}, but not to the TMTV. Therefore, while the metabolic profile of the tumour is complex and might differ at the single-cell level,[45] our findings suggest that the total amount of intratumoural B- and T-cells plays a less significant role in the pre-treatment ^{18}FDG-PET/CT metrics in DLBCL.

Cell-mediated immunity plays a crucial role in controlling tumour growth and progression, including in DLBCL.[46] In line with our study, previous studies utilizing FCM-based quantification methods also showed higher levels of

CD4+ cell infiltration, but not CD8+ cell infiltration, which is associated with favourable outcomes in DLBCL.[31, 33] Furthermore, the determined cut-off value of TI CD4+ cells (24%) in the current study is approximate to that of previous studies (20% and 23%). However, the reason why an abundance of CD4+ cells is associated with a good prognosis and which functional subpopulation mainly contributes to a favourable prognosis is not fully understood. One study discussed the responsibility of memory CD4+/CD45RO+ T-cells,[33] whereas others demonstrated the beneficial impact of higher intratumoural CD4+/FOXP3+ regulatory T-cells on DLBCL.[47] CD4+ T-cells primarily activate other immune cells including CD8+ T-cells rather directly eradicate tumor cells as effector T-cells.[48] Given this hierarchical role in immune interaction, one possible explanation is that the prevalence of CD4+ cells within tumours may simply serve as a surrogate marker for a more efficient local immune surveillance.[33]

The strength of our study lies in the use of diagnostic modalities with easily derived parameters, allowing for rapid and straightforward implementation in clinical practice. However, several limitations need to be addressed in subsequent studies. First, the retrospective nature of the study design and the treatment heterogeneity (R-CHOP or R-CHOP-like regimen) in patients precluded us from drawing definitive conclusions. Second, the cohort size was relatively small, and only cases with sufficient tissue sampling were analysed, which may have contributed to bias in the selection of cases. It should be noted that a large number of patients who faced challenges obtaining sufficient biopsy samples, especially those with predominantly extranodal lesions, were excluded from our cohort. Third, the phenotypic and functional diversity of intratumoural cells was not evaluated. Given the heterogeneity of CD4+ T-cells, which can exhibit either suppressive or promotive effects on tumour immunity, a sole reliance on quantitative T-cell analysis may not yield a comprehensive understanding. The dysfunctional state known as T-cell exhaustion, marked by increased inhibitory receptors and decreased effector cytokines,[49] has been increasingly recognized for its prognostic significance in DLBCL.[25, 26, 29] Other immune cells, such as tumour-associated macrophages and dendritic cells, appear to establish a cross-talk with neoplastic cells and the tumour microenvironment.[24, 50] Finally, the cell infiltration ratio derived from cell suspensions may not accurately represent the actual cell ratio observed by immunohistochemistry (IHC) and could be overestimated.[51] Nevertheless, IHC-based quantification is time-consuming, costly, and importantly method-dependent, which may lead to a higher risk of conflicting results.[52] From this perspective, easily obtainable and reproducible cell counting through FCM is suitable for routine use to complement TMTV-based risk prediction.

In conclusion, our study revealed that both high TMTV and low TI CD4+ cells were independently associated with poor prognosis in newly diagnosed DLBCL. The combined use of these parameters more effectively distinguished outcomes between individuals within the same IPI 0-2 or 3-5 categories. This study underscores the need for simultaneous assessment of both tumour volume and tumour composition to augment the TMTV-based stratification systems.

References

1. Sehn LH, Salles G. Diffuse Large B-Cell Lymphoma. N Engl J Med. 2021;384(9):842-858.
2. Chapuy B, Stewart C, Dunford AJ, et al. Molecular subtypes of diffuse large B cell lymphoma are associated with distinct pathogenic mechanisms and outcomes. Nat Med. 2018;24(5):679-690.
3. Westin J, Sehn LH. CAR T cells as a second-line therapy for large B-cell lymphoma: a paradigm shift? Blood. 2022;139(18):2737-2746.
4. Falchi L, Vardhana SA, Salles GA. Bispecific antibodies for the treatment of B-cell lymphoma: promises, unknowns, and opportunities. Blood. 2023;141(5):467-480.
5. International Non-Hodgkin's Lymphoma Prognostic Factors Project. A predictive model for aggressive non-Hodgkin's lymphoma. N Engl J Med. 1993;329(14):987-994.
6. Sehn LH, Berry B, Chhanabhai M, et al. The revised International Prognostic Index (R-IPI) is a better predictor of outcome than the standard IPI for patients with diffuse large B-cell lymphoma treated with R-CHOP. Blood. 2007;109(5):1857-1861.
7. Zhou Z, Sehn LH, Rademaker AW, et al. An enhanced International Prognostic Index (NCCN-IPI) for patients with diffuse large B-cell lymphoma treated in the rituximab era. Blood. 2014;123(6):837-842.
8. Wright GW, Huang DW, Phelan JD, et al. A Probabilistic Classification Tool for Genetic Subtypes of Diffuse Large B Cell Lymphoma with Therapeutic Implications. Cancer Cell. 2020;37(4):551-568.e14.
9. Ennishi D, Jiang A, Boyle M, et al. Double-Hit Gene Expression Signature Defines a Distinct Subgroup of Germinal Center B-Cell-Like Diffuse Large B-Cell Lymphoma. J Clin Oncol. 2019;37(3):190-201.
10. Urata T, Naoi Y, Jiang A, et al. Distribution and clinical impact of molecular subtypes with Dark Zone signature of DLBCL in a Japanese real-world study. Blood Adv. 2023;7(24):7459-7470.
11. Zhang MC, Tian S, Fu D, et al. Genetic subtype-guided immunochemotherapy in diffuse large B cell lymphoma: The randomized GUIDANCE-01 trial. Cancer Cell. 2023;41(10):1705-1716.e5.
12. Nanni C, Kobe C, Baessler B, et al. European Association of Nuclear Medicine (EANM) Focus 4 consensus recommendations: molecular imaging and therapy in haematological tumours. Lancet Haematol. 2023;10(5):e367-e381.
13. Senjo H, Hirata K, Izumiyama K, et al. High metabolic heterogeneity on baseline 18FDG-PET/CT scan as a poor prognostic factor for newly diagnosed diffuse large B-cell lymphoma. Blood Adv. 2020;4(10):2286-2296.
14. Ceriani L, Gritti G, Cascione L, et al. SAKK38/07 study: integration of baseline metabolic heterogeneity and metabolic tumor volume in DLBCL prognostic model. Blood Adv. 2020;4(6):1082-1092.
15. Kidd EA, Grigsby PW. Intratumoral metabolic heterogeneity of cervical cancer. Clin Cancer Res. 2008;14(16):5236-5241.
16. El-Galaly TC, Villa D, Cheah CY, Gormsen LC. Pre-treatment total metabolic tumour volumes in lymphoma: Does quantity matter? Br J Haematol. 2022;197(2):139-155.
17. Eude F, Toledano MN, Vera P, Tilly H, Mihailescu SD, Becker S. Reproducibility of Baseline Tumour Metabolic Volume Measurements in Diffuse Large B-Cell LymphomA: Is There a Superior Method? Metabolites. 2021;11(2):72.

18. Kostakoglu L, Mattiello F, Martelli M, et al. Total metabolic tumor volume as a survival predictor for patients with diffuse large B-cell lymphoma in the GOYA study. Haematologica. 2022;107(7):1633-1642.
19. Vercellino L, Cottereau AS, Casasnovas O, et al. High total metabolic tumor volume at baseline predicts survival independent of response to therapy. Blood. 2020;135(16):1396-1405.
20. Eertink JJ, Zwezerijnen GJC, Heymans MW, et al. Baseline PET radiomics outperforms the IPI risk score for prediction of outcome in diffuse large B-cell lymphoma. Blood. 2023;141(25):3055-3064.
21. Le Goff E, Blanc-Durand P, et al. Baseline circulating tumour DNA and total metabolic tumour volume as early outcome predictors in aggressive large B-cell lymphoma. A real-world 112-patient cohort. Br J Haematol. 2023;202(1):54-64.
22. Liu C, Shi P, Li Z, Li B, Li Z. A nomogram for predicting the rapid progression of diffuse large B-cell lymphoma established by combining baseline PET/CT total metabolic tumor volume, lesion diffusion, and TP53 mutations. Cancer Med. 2023;12(16):16734-16743.
23. Toledano MN, Desbordes P, Banjar A, et al. Combination of baseline FDG PET/CT total metabolic tumour volume and gene expression profile have a robust predictive value in patients with diffuse large B-cell lymphoma. Eur J Nucl Med Mol Imaging. 2018;45(5):680-688.
24. Autio M, Leivonen SK, Bruck O, Karjalainen-Lindsberg ML, Pellinen T, Leppa S. Clinical Impact of Immune Cells and Their Spatial Interactions in Diffuse Large B-Cell Lymphoma Microenvironment. Clin Cancer Res. 2022;28(4):781-792.
25. Roussel M, Le KS, Granier C, et al. Functional characterization of PD1+TIM3+ tumor-infiltrating T cells in DLBCL and effects of PD1 or TIM3 blockade. Blood Adv. 2021;5(7):1816-1829.
26. Autio M, Leivonen SK, Bruck O, et al. Immune cell constitution in the tumor microenvironment predicts the outcome in diffuse large B-cell lymphoma. Haematologica. 2021;106(3):718-729.
27. Xu-Monette ZY, Xiao M, Au Q, et al. Immune Profiling and Quantitative Analysis Decipher the Clinical Role of Immune-Checkpoint Expression in the Tumor Immune Microenvironment of DLBCL. Cancer Immunol Res. 2019;7(4):644-657.
28. Ennishi D, Takata K, Beguelin W, et al. Molecular and Genetic Characterization of MHC Deficiency Identifies EZH2 as Therapeutic Target for Enhancing Immune Recognition. Cancer Discov. 2019;9(4):546-563.
29. Song JY, Nwangwu M, He TF, et al. Low T-cell proportion in the tumor microenvironment is associated with immune escape and poor survival in diffuse large B-cell lymphoma. Haematologica. 2023;108(8):2167-2177.
30. Coutinho R, Clear AJ, Mazzola E, et al. Revisiting the immune microenvironment of diffuse large B-cell lymphoma using a tissue microarray and immunohistochemistry: robust semi-automated analysis reveals CD3 and FoxP3 as potential predictors of response to R-CHOP. Haematologica. 2015;100(3):363-369.
31. Keane C, Gill D, Vari F, Cross D, Griffiths L, Gandhi M. CD4(+) tumor infiltrating lymphocytes are prognostic and independent of R-IPI in patients with DLBCL receiving R-CHOP chemo-immunotherapy. Am J Hematol. 2013;88(4):273-276.
32. Leivonen SK, Pollari M, Bruck O, et al. T-cell inflamed tumor microenvironment predicts favorable prognosis in primary testicular lymphoma. Haematologica. 2019;104(2):338-346.

33. Ansell SM, Stenson M, Habermann TM, Jelinek DF, Witzig TE. Cd4+ T-cell immune response to large B-cell non-Hodgkin's lymphoma predicts patient outcome. J Clin Oncol. 2001;19(3):720-726.
34. Terao T, Machida Y, Hirata K, et al. Prognostic Impact of Metabolic Heterogeneity in Patients With Newly Diagnosed Multiple Myeloma Using 18F-FDG PET/CT. Clin Nucl Med. 2021;46(10):790-796.
35. Hans CP, Weisenburger DD, Greiner TC, et al. Confirmation of the molecular classification of diffuse large B-cell lymphoma by immunohistochemistry using a tissue microarray. Blood. 2004;103(1):275-282.
36. Nowakowski GS, Chiappella A, Witzig TE, et al. Variable global distribution of cell-of-origin from the ROBUST phase III study in diffuse large B-cell lymphoma. Haematologica. 2020;105(2):e72-e75.
37. Urata T, Naoi Y, Jiang A, et al. Distribution and clinical impact of molecular subtypes with dark zone signature of DLBCL in a Japanese real-world study. Blood Adv. 2023;7(24):7459-7470.
38. Kataoka K, Miyoshi H, Sakata S, et al. Frequent structural variations involving programmed death ligands in Epstein-Barr virus-associated lymphomas. Leukemia. 2019;33(7):1687-1699.
39. Mikhaeel NG, Heymans MW, Eertink JJ, et al. Proposed New Dynamic Prognostic Index for Diffuse Large B-Cell Lymphoma: International Metabolic Prognostic Index. J Clin Oncol. 2022;40(21):2352-2360.
40. Dayde D, Ternant D, Ohresser M, et al. Tumor burden influences exposure and response to rituximab: pharmacokinetic-pharmacodynamic modeling using a syngeneic bioluminescent murine model expressing human CD20. Blood. 2009;113(16):3765-3772.
41. Tout M, Casasnovas O, Meignan M, et al. Rituximab exposure is influenced by baseline metabolic tumor volume and predicts outcome of DLBCL patients: a Lymphoma Study Association report. Blood. 2017;129(19):2616-2623.
42. Vercellino L, Di Blasi R, Kanoun S, et al. Predictive factors of early progression after CAR T-cell therapy in relapsed/refractory diffuse large B-cell lymphoma. Blood Adv. 2020;4(22):5607-5615.
43. Rojek AE, Kline JP, Feinberg N, et al. Optimization of Metabolic Tumor Volume as a Prognostic Marker in CAR T-Cell Therapy for Aggressive Large B-cell NHL. Clin Lymphoma Myeloma Leuk. 2024;24(2):83-93.
44. Nath K, Law SC, Sabdia MB, et al. Intratumoral T cells have a differential impact on FDG-PET parameters in follicular lymphoma. Blood Adv. 2021;5(12):2644-2649.
45. Huang B, Chan T, Kwong DL, Chan WK, Khong PL. Nasopharyngeal carcinoma: investigation of intratumoral heterogeneity with FDG PET/CT. AJR Am J Roentgenol. 2012;199(1):169-174.
46. Tamma R, Ranieri G, Ingravallo G, et al. Inflammatory Cells in Diffuse Large B Cell Lymphoma. J Clin Med. 2020;9(8):2418.
47. Chang C, Chen YP, Medeiros LJ, Chen TY, Chang KC. Higher infiltration of intratumoral CD25+ FOXP3+ lymphocytes correlates with a favorable prognosis in patients with diffuse large B-cell lymphoma. Leuk Lymphoma. 2021;62(1):76-85.
48. Kruse B, Buzzai AC, Shridhar N, et al. CD4(+) T cell-induced inflammatory cell death controls immune-evasive tumours. Nature. 2023;618(7967):1033-1040.
49. Jiang Y, Li Y, Zhu B. T-cell exhaustion in the tumor microenvironment. Cell Death Dis. 2015;6(6):e1792.
50. Chang KC, Huang GC, Jones D, Lin YH. Distribution patterns of dendritic cells and T cells in diffuse large B-cell lymphomas correlate with prognoses. Clin Cancer Res. 2007;13(22 Pt 1):6666-6672.

51. Xu Y, Kroft SH, McKenna RW, Aquino DB. Prognostic significance of tumour-infiltrating T lymphocytes and T-cell subsets in de novo diffuse large B-cell lymphoma: a multiparameter flow cytometry study. Br J Haematol. 2001;112(4):945-949.

52. Miyawaki K, Sugio T. Lymphoma Microenvironment in DLBCL and PTCL-NOS: the key to uncovering heterogeneity and the potential for stratification. J Clin Exp Hematop. 2022;62(3):127-135.

Table 1. Clinical characteristics of included patients according to tumour-infiltrating CD4+ cell levels

	Total (n=171 [100%])	Patients with high TI-CD4+ cells (n=95 [55.6%])	Patients with low TI-CD4+ cells (n=76 [44.4%])	P
Age, year, median (IQR)	71 (61-79)	70 (62-78)	71 (61-79)	0.856
Age >60, n (%)	130 (76.0)	72 (75.8)	58 (76.3)	1
Female, n (%)	80 (46.7)	43 (45.3)	37 (48.7)	0.758
ECOGPS ≧2, n (%)	37 (21.4)	26 (27.4)	11 (14.5)	0.065
LDH >UNL, n (%)	116 (67.8)	64 (67.4)	51 (67.1)	1
Ann Arbor stage ≧3, n (%)	101 (59.1)	60 (63.2)	41 (53.9)	0.533
Number of EN lesions ≧2, n (%)	38 (22.2)	21 (22.1)	17 (22.4)	1
IPI, n (%)				
0-2	89 (52.0)	47 (49.5)	42 (55.3)	-
3-5	82 (48.0)	48 (50.5)	34 (44.7)	0.549
Disease type, n (%)				
DLBCL, NOS	156 (91.2)	82 (86.3)	74 (97.4)	0.013
t-FL	8 (4.7)	6 (6.3)	2 (2.6)	0.302
EBV-positive DLBCL	7 (4.1)	7 (7.4)	0 (0)	0.017
COO according to Hans algorithm, n (%)				
GCB type	48 (28.1)	25 (26.3)	23 (30.3)	0.647
non-GCB type	89 (52.0)	51 (53.7)	38 (50.0)	0.61
Missing	34 (19.9)	19 (20.0)	15 (19.7)	1
TMTV, median mL (IQR)	177.8 (47-560)	170.7 (29.5-536)	188 (73.1-646.4)	0.169
Cellular contents in tumor, median % (IQR)				
CD19+ cells	41.5 (20.5-60.3)	25.9 (12.7-40.5)	60.7 (46-74.9)	<0.001

CD3+ cells	49.8 (29.5-67.6)	65.4 (51.3-77.5)	23.1 (13.1-39.7)	<0.001
CD4+ cells	26.3 (13.8-42.7)	39.3 (31.7-52)	11.8 (5.9-19.2)	<0.001
CD8+ cells	16.2 (9.5-23.1)	18.2 (11.5-25)	12.4 (6.8-20.5)	0.002
Induction regimen, n (%)				
R-CHOP	149 (87.1)	82 (86.3)	67 (88.2)	0.82
More intensive chemotherapy	13 (7.6)	5 (5.2)	8 (10.5)	0.25
Less intensive chemotherapy	9 (5.3)	8 (8.4)	1 (1.3)	0.044
CR achievement at end of induction, n (%)	139 (81.3)	81 (85.3)	58 (76.3)	0.168

Abbreviations: TI, tumor-infiltrating; IQR, interquartile range; ECOGPS, European Cooperative Oncology Group Performance Status; LDH, lactate dehydrogenase; UNL, upper normal limit; EN, extranodal; IPI, International Prognostic Index; DLBCL, NOS, diffuse large B-cell lymphoma, not otherwise specified; t-FL,DLBCL transformed from follicular lymphoma; EBV, Epstein-Barr virus; COO, cell of origin; GCB, germinal center B-cell; TMTV, total metabolic tumor volume; R-CHOP, rituximab combined with cyclophosphamide, doxorubicin, vincristine, and prednisone; CR, complete remission.

1

Table 2. Univariate and multivariate analysis for predicting PFS and OS

	PFS						OS					
	Univariate			Multivariate			Univariate			Multivariate		
	HR	95% CI	P	HR	95% CI	P	HR	95% CI	P	HR	95% CI	P
Age >60	3.12	1.6-6.07	0.001	–	–	–	2.82	1.41-5.79	0.003	–	–	–
ECOGPS ≧2	2.79	1.73-4.48	<0.001	–	–	–	3.22	1.94-5.36	<0.001	–	–	–
LDH >UNL	2.25	1.31-3.84	0.003	–	–	–	2.21	1.23-3.99	0.008	–	–	–
Ann Arbor stage ≧3	1.6	1.01-2.54	0.042	–	–	–	1.28	0.78-2.09	0.32	–	–	–
Number of EN lesions ≧2	2.25	1.4-3.63	0.001	–	–	–	2.16	1.3-3.61	0.003	–	–	–
Intensive chemotherapy	0.55	0.2-1.51	0.251	–	–	–	0.75	0.27-2.07	0.585	–	–	–
Cell of origin*, non-GCB	1.33	0.78-2.28	0.29	–	–	–	1.4	0.77-2.56	0.261	–	–	–
IPI 3-5	2.64	1.67-4.17	<0.001	1.97	1.13-3.42	0.016	2.39	1.46-3.92	0.001	1.75	0.96-3.21	0.068
Low CD4+ cells	1.64	1.05-2.54	0.027	1.69	1.09-2.62	0.018	2.09	1.29-3.4	0.003	2.15	1.32-3.5	0.002
High TMTV	2.59	1.67-4.02	<0.001	1.76	1.03-3	0.036	2.56	1.58-4.15	<0.001	1.85	1.02-3.34	0.04

Abbreviation: PFS, progression free survival; OS, overall survival; R-ISS, revised-international staging system; ECOGPS, Eastern Cooperative Oncology Group Performance Status; LDH, lactate dehydrogenase; UNL, upper normal limit; EN, extranodal; GCB, germinal center B-cell type; IPI, international prognostic index; TMTV, total metabolic tumor volume; HR, hazard ratio; CI, confidence interval.

* The cell of origin was evaluable in 137 patients according to the Hans algorithm.

Figure legends

Figure 1: Schematic representation of the calculation of functional PET/CT parameters and the gating strategy for intratumoural cellular contents

A) An example of a patient with a high tumour burden. The red areas represent lymphoma lesions used for calculating the TMTV. Physiological uptakes, such as those in the tonsils and urinary tract, are manually excluded and marked in blue. The yellow circle indicates the biopsied lymph node from which lesion radiomic parameters and cellular composition are subsequently measured. B) The gating strategy for quantifying cellular content within biopsied samples. The left panel shows the distinction between CD19+ and CD19- lymphocytes, while the right panel identifies the CD4/CD8 expression pattern.

Abbreviations: TMTV, total metabolic tumour volume; SUV, standardized uptake value; TLG, total lesion glycolysis.

Figure 2: Relationship between functional PET/CT parameters and the proportions of intratumoural cellular components

The correlation between the proportions of intratumoural CD19+, CD3+, CD4+, and CD8+ cells (represented by blue, yellow, grey, and brown dots, respectively) and A) SUV_{max}, B) TMTV, and C) TLG is illustrated with regression lines and a 95% confidence interval (shaded area). D) The heatmap representing correlation plots between radiomic and cellular parameters. Each square represents the correlation coefficients (R values) between the variables on its axes, with a cross mark indicating no statistical significance.

Abbreviations: TMTV, total metabolic tumour volume; SUV, standardized uptake value; TLG, total lesion glycolysis; ns, not significant.

Figure 3: Kaplan–Meier estimates of PFS and OS based on intratumoural CD4+ cell levels and TMTV values

A) PFS and B) OS according to intratumoural CD4+ cell levels. C) PFS and D) OS according to TMTV values.

Abbreviations: TMTV, total metabolic tumour volume.

Figure 4: Survival analysis stratified by the combination of tumour-infiltrating CD4+ cells and TMTV

Kaplan-Meier estimates of A) PFS and B) OS using the combined model. * and ** represent P-values of <0.05 and <0.01, respectively.

Abbreviations: TMTV, total metabolic tumour volume; ns, not significant.

Figure 5: Integration of intratumoural CD4+ burden and TMTV into the IPI system

A) Receiver operating curve for predicting 3-year survival based on IPI, CD4+ intratumoural cells, TMTV, and their combination as continuous variables. * and ** represent P-values of <0.05 and <0.01, respectively. B) Alluvial diagram representing the transition of ISS category to risk factor number-based classification. C) PFS and D) OS according to the number of risk factors (IPI 3-5, high TMTV, and low CD4+ cells in tumour).

Abbreviations: IPI, international prognostic index; TMTV, total metabolic tumour volume; ISS, international staging system; AUC, area under the curve; SE, sensitivity; SP, specificity.

A

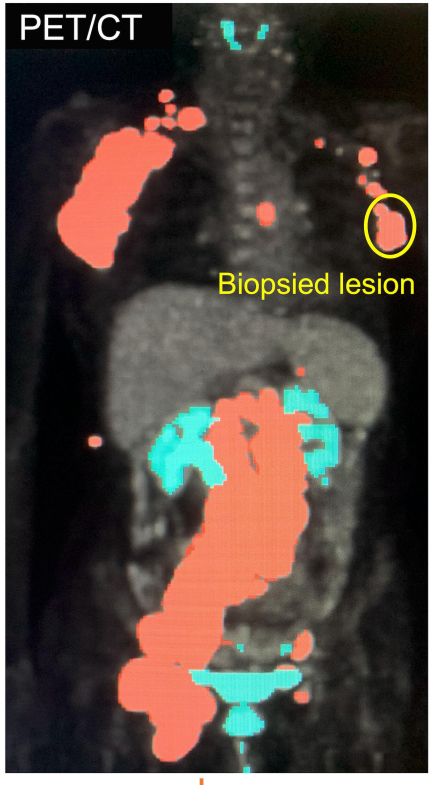

② Measure lesional PET/CT parameters

1) Lesional SUVmax (SUV_{lesion})
2) SUVmean
3) Lesional MTV (MTV_{lesion})
4) Lesional TLG (TLG_{lesion})

③ Calculate % CD19+, CD3+, CD4+ and CD8+ cells

① Calculate TMTV

TMTV =1385 mL ⇨ High TMTV

B

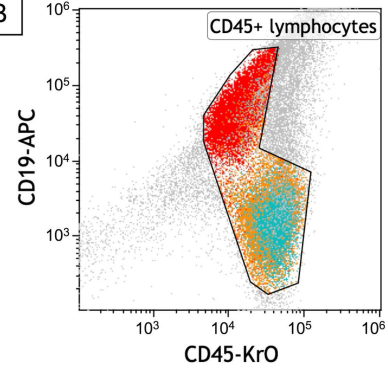

Gate	Number	%Total
All	50,000	100.00
CD45+ lymphocytes	41,333	82.67

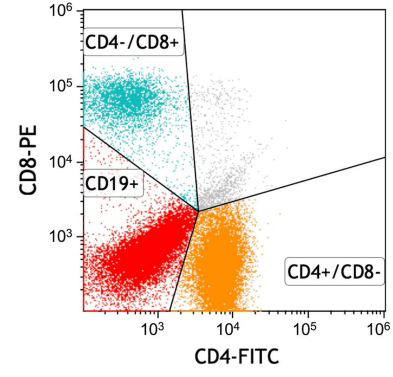

Gate	Number	%Total	%Gated
All	41,333	82.67	100.00
CD19+	15,964	31.93	38.62
CD4-/CD8+	4,455	8.91	10.78
CD4+/CD8-	19,832	39.66	47.98

%CD4+ =47.98 % ⇨ High CD4+ cells

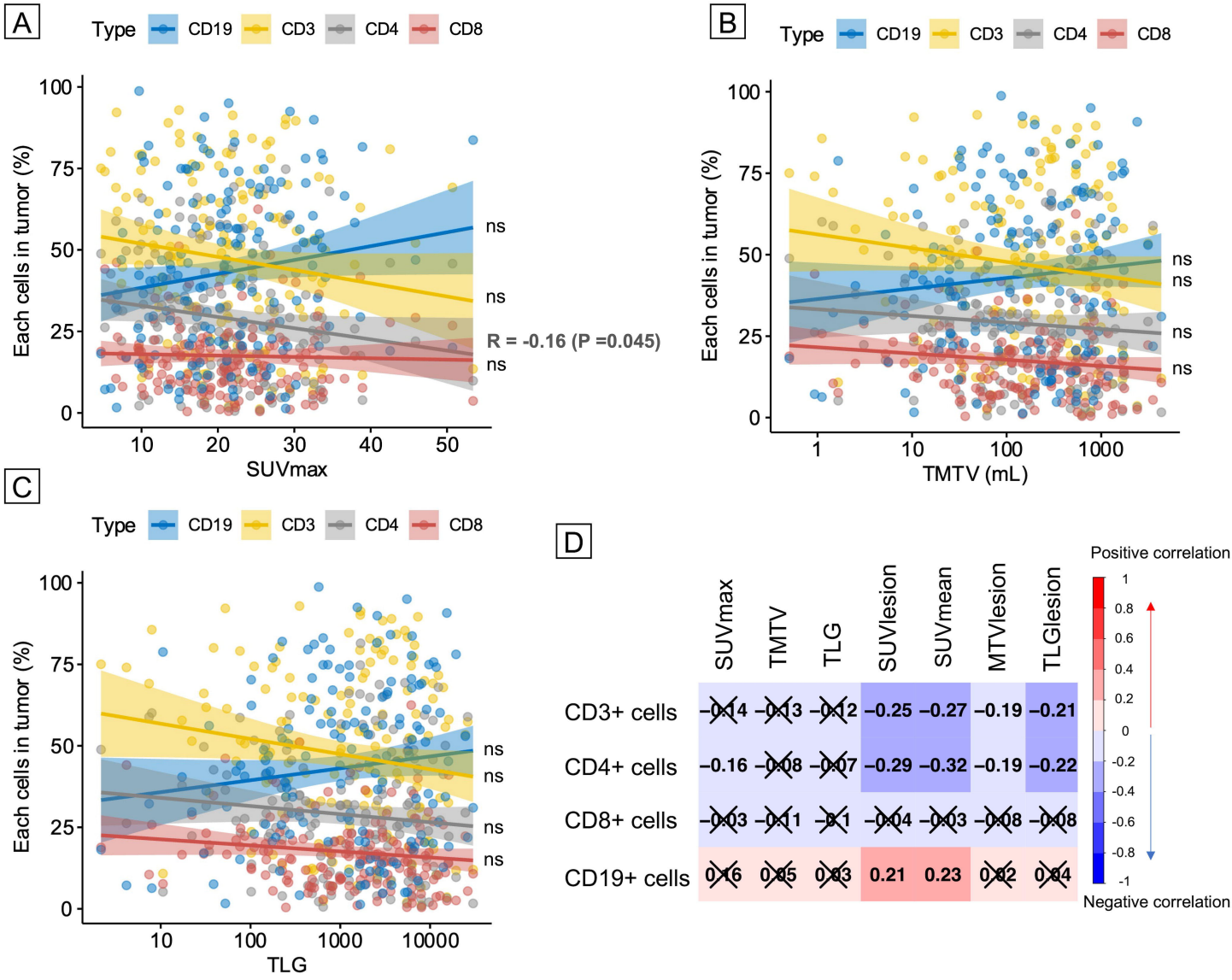
A
Type
CD19
CD3
CD4
CD8
Each cells in tumor (%)
SUVmax
ns
ns
R = -0.16 (P =0.045)
ns
B
TMTV (mL)
C
TLG
D
SUVmax
TMTV
TLG
SUVlesion
SUVmean
MTVlesion
TLGlesion
CD3+ cells
CD4+ cells
CD8+ cells
CD19+ cells
Positive correlation
Negative correlation

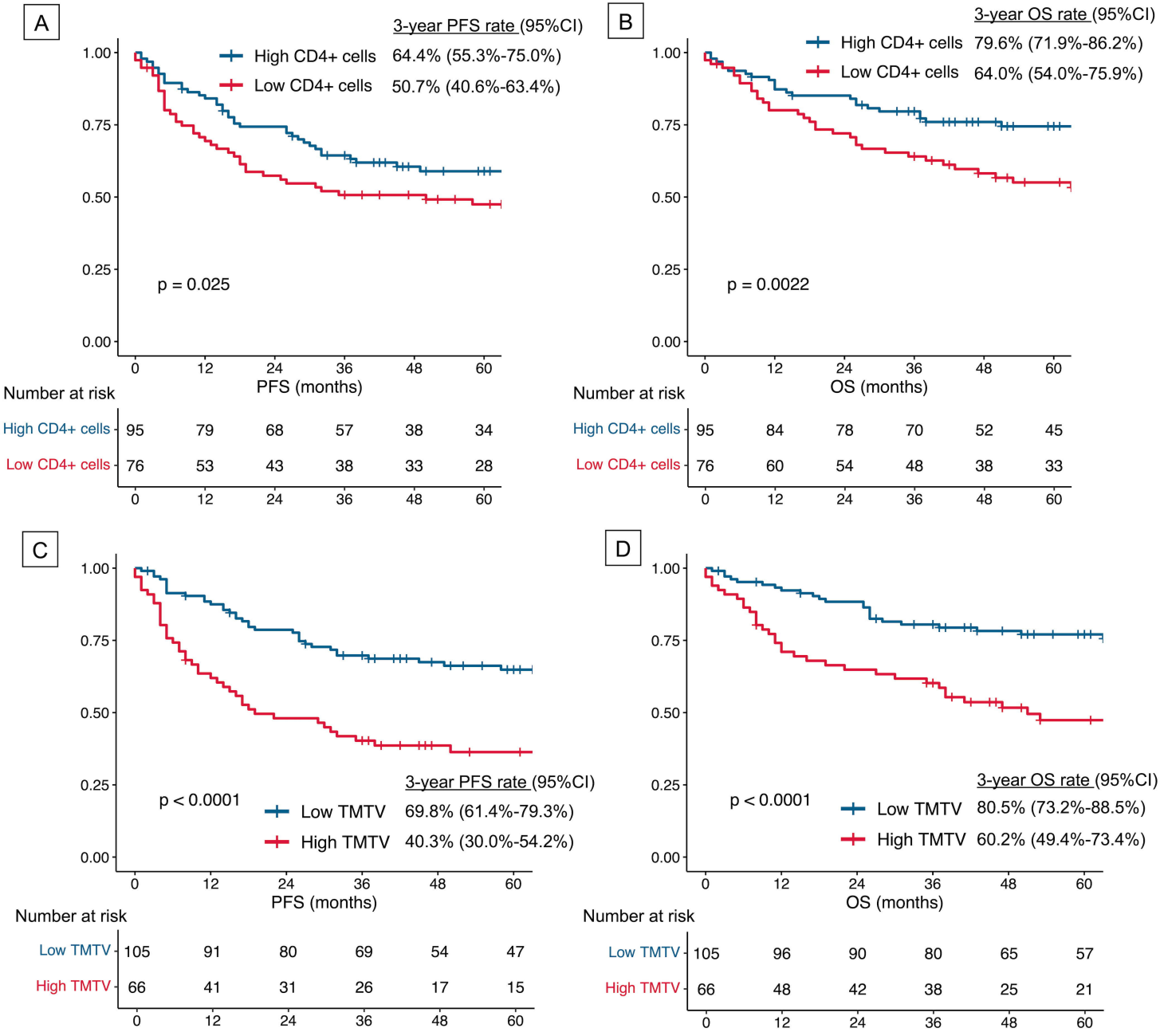
A
3-year PFS rate (95%CI)
High CD4+ cells 64.4% (55.3%-75.0%)
Low CD4+ cells 50.7% (40.6%-63.4%)
p = 0.025
PFS (months)
Number at risk
High CD4+ cells 95 79 68 57 38 34
Low CD4+ cells 76 53 43 38 33 28
B
3-year OS rate (95%CI)
High CD4+ cells 79.6% (71.9%-86.2%)
Low CD4+ cells 64.0% (54.0%-75.9%)
p = 0.0022
OS (months)
Number at risk
High CD4+ cells 95 84 78 70 52 45
Low CD4+ cells 76 60 54 48 38 33
C
p < 0.0001
3-year PFS rate (95%CI)
Low TMTV 69.8% (61.4%-79.3%)
High TMTV 40.3% (30.0%-54.2%)
PFS (months)
Number at risk
Low TMTV 105 91 80 69 54 47
High TMTV 66 41 31 26 17 15
D
p < 0.0001
3-year OS rate (95%CI)
Low TMTV 80.5% (73.2%-88.5%)
High TMTV 60.2% (49.4%-73.4%)
OS (months)
Number at risk
Low TMTV 105 96 90 80 65 57
High TMTV 66 48 42 38 25 21

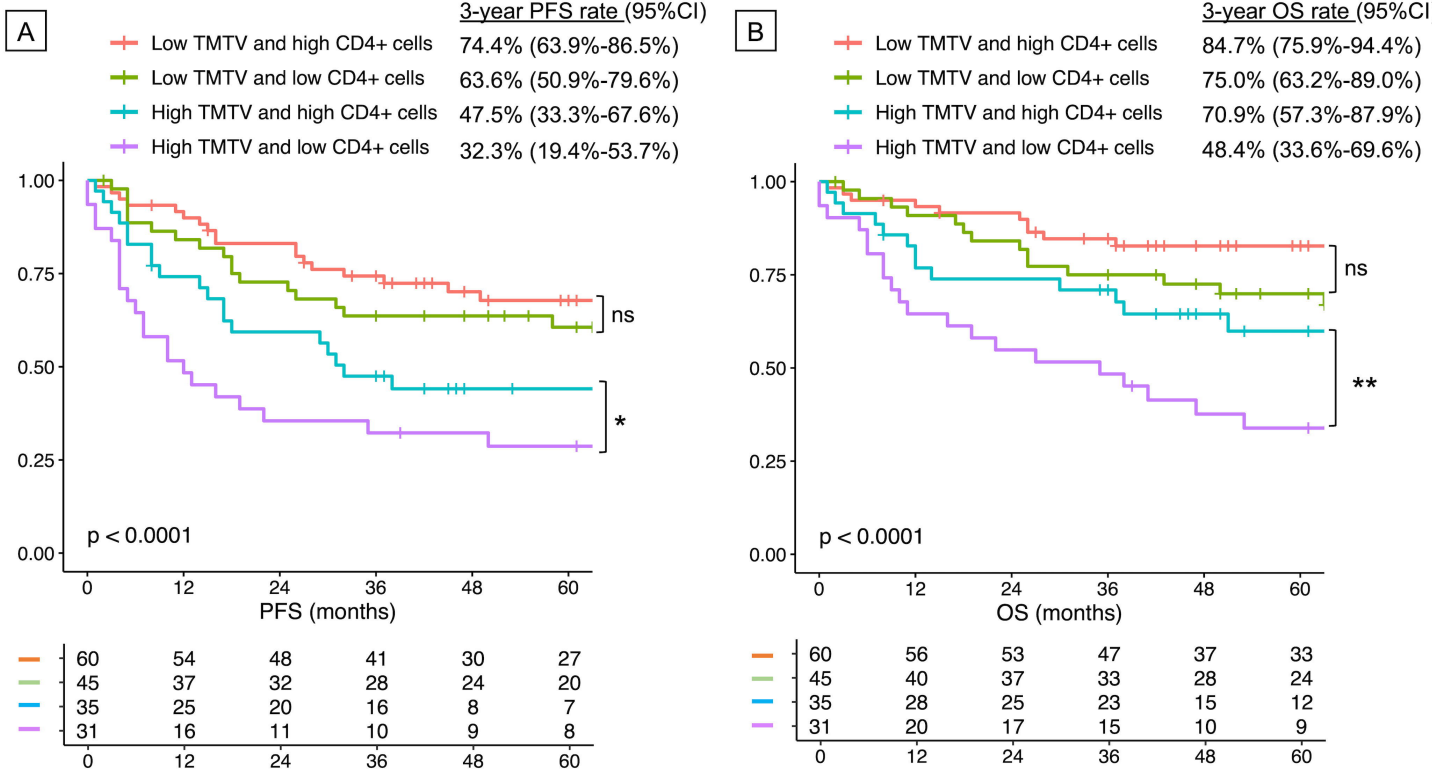
A
3-year PFS rate (95%CI)
Low TMTV and high CD4+ cells
74.4% (63.9%-86.5%)
Low TMTV and low CD4+ cells
63.6% (50.9%-79.6%)
High TMTV and high CD4+ cells
47.5% (33.3%-67.6%)
High TMTV and low CD4+ cells
32.3% (19.4%-53.7%)
1.00
0.75
0.50
0.25
0.00
ns
*
p < 0.0001
0
12
24
36
48
60
PFS (months)
60 54 48 41 30 27
45 37 32 28 24 20
35 25 20 16 8 7
31 16 11 10 9 8
0
12
24
36
48
60
B
3-year OS rate (95%CI)
Low TMTV and high CD4+ cells
84.7% (75.9%-94.4%)
Low TMTV and low CD4+ cells
75.0% (63.2%-89.0%)
High TMTV and high CD4+ cells
70.9% (57.3%-87.9%)
High TMTV and low CD4+ cells
48.4% (33.6%-69.6%)
1.00
0.75
0.50
0.25
0.00
ns
**
p < 0.0001
0
12
24
36
48
60
OS (months)
60 56 53 47 37 33
45 40 37 33 28 24
35 28 25 23 15 12
31 20 17 15 10 9
0
12
24
36
48
60

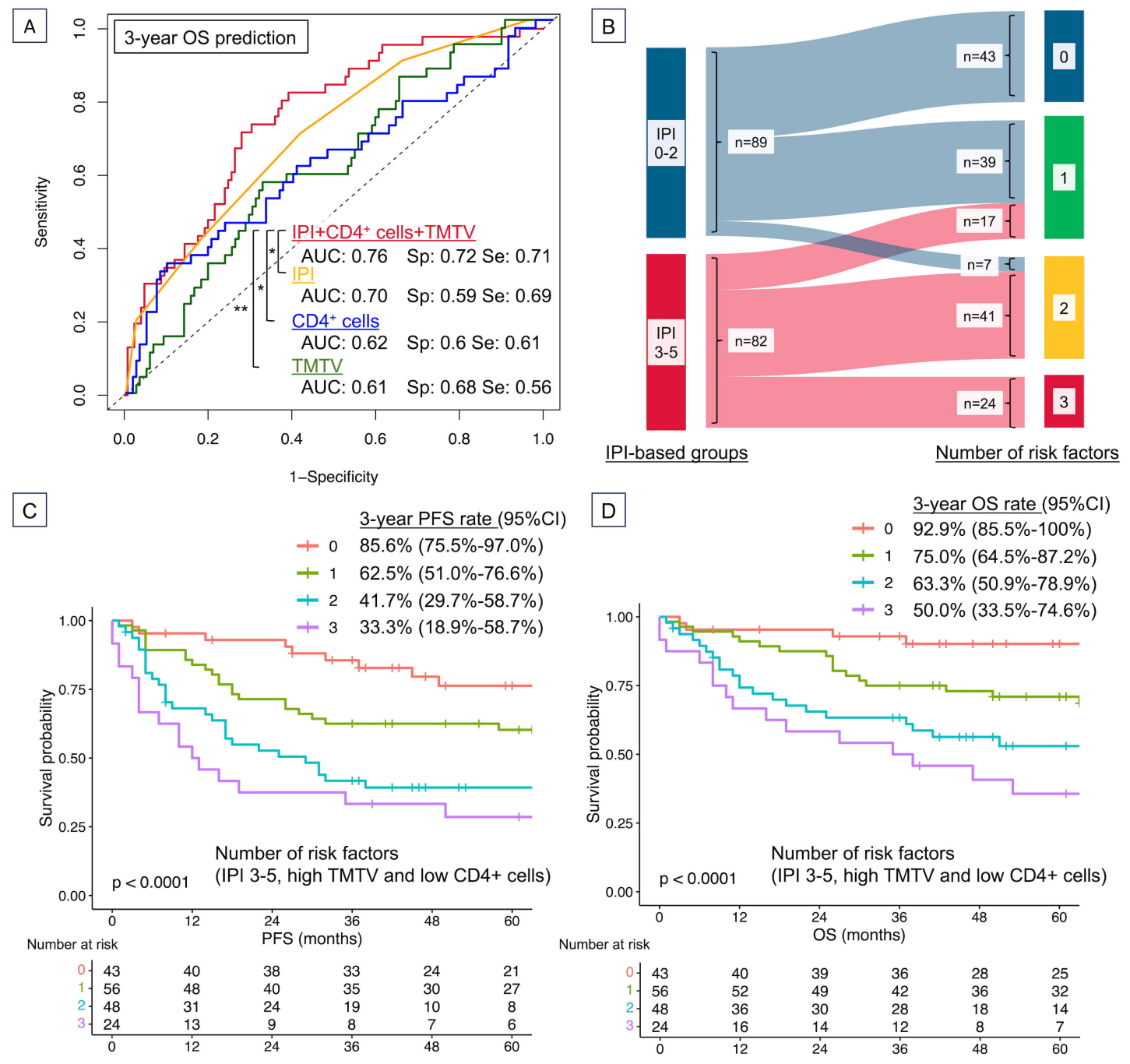
A
3-year OS prediction
Sensitivity
1−Specificity
IPI+CD4⁺ cells+TMTV
AUC: 0.76 Sp: 0.72 Se: 0.71
IPI
AUC: 0.70 Sp: 0.59 Se: 0.69
CD4⁺ cells
AUC: 0.62 Sp: 0.6 Se: 0.61
TMTV
AUC: 0.61 Sp: 0.68 Se: 0.56
B
IPI 0-2
IPI 3-5
n=89
n=82
n=43
n=39
n=17
n=7
n=41
n=24
0
1
2
3
IPI-based groups
Number of risk factors
C
3-year PFS rate (95%CI)
0 85.6% (75.5%-97.0%)
1 62.5% (51.0%-76.6%)
2 41.7% (29.7%-58.7%)
3 33.3% (18.9%-58.7%)
Survival probability
p < 0.0001
Number of risk factors
(IPI 3-5, high TMTV and low CD4+ cells)
PFS (months)
Number at risk
0 43 40 38 33 24 21
1 56 48 40 35 30 27
2 48 31 24 19 10 8
3 24 13 9 8 7 6
D
3-year OS rate (95%CI)
0 92.9% (85.5%-100%)
1 75.0% (64.5%-87.2%)
2 63.3% (50.9%-78.9%)
3 50.0% (33.5%-74.6%)
Survival probability
p < 0.0001
Number of risk factors
(IPI 3-5, high TMTV and low CD4+ cells)
OS (months)
Number at risk
0 43 40 39 36 28 25
1 56 52 49 42 36 32
2 48 36 30 28 18 14
3 24 16 14 12 8 7

Supplementary methods

Patient cohort and study design

We conducted a retrospective analysis of newly diagnosed patients with histologically confirmed DLBCL who were treated with rituximab (RTX) plus cyclophosphamide (CY), doxorubicin (DXR), vincristine (VCR), and prednisone (PSL) (R-CHOP) or R-CHOP-like chemotherapy at Kameda Medical Center between 2006 and 2020. The R-CHOP-like regimen was categorized as either a more intensive chemotherapy, defined as RTX combined with etoposide, PSL, VCR, CY, and DXR (R-EPOCH), or hyperfractionated CY, VCR, DXR and dexamethasone (R-HyperCVAD), or a less intensive treatment such as R-CHOP without DXR (R-CVP) or without VCR (R-CHP). The primary exclusion criteria were the absence of pre-treatment PET/CT with FDG-avid lesions and the insufficient flow cytometric (FCM) data from biopsied lymphoma lesions. Patients with high-grade B-cell lymphoma harbouring concurrent rearrangements of *MYC*, *BCL2*, or *BCL6* were also excluded. Patients with untreated histologically transformed follicular lymphoma (tFL) and Epstein-Barr virus (EBV)-positive DLBCL were not excluded. No cases of T-cell/histiocyte-rich large B-cell lymphoma pathologically confirmed were observed in the entire cohort. The DLBCL cell of origin was determined using immunohistochemistry (IHC) according to the Hans algorithm.[1] The pathological diagnosis was made by expert haematopathologists according to the 2016 revision of the World Health Organization classification.[2] The response to first-line treatment was evaluated at the end of induction based on the Lugano 2014 criteria.[3] The flow diagram of patient enrolment is shown in Supplementary Figure 1. Due to the large number of patients excluded because of unavailable or inappropriate FCM data, baseline clinical characteristics were compared between those with and without FCM data (Supplementary Table 1). All clinical factors were not significantly different, except for the older age in patients excluded from the analysis (median 74 vs. 71 years, P=0.006). Unexpectedly, patients who were not able to obtain sufficient samples for FCM were significantly more likely to have biopsies from extranodal lesions (54.7% vs. 15.8%, P <0.001), including the gastrointestinal (GI) tract. Concerning clinical outcomes, the 171 included and 347 excluded patients showed comparable 3-year progression free survival (PFS) (58.3% 95% confidence interval [CI]: 51.3%-66.3% vs. 61.4% 95% CI: 56.2%-67.0%, P = 0.35) and OS rates (72.6% 95% CI: 66.2%-79.7% vs. 68.5% 95% CI 63.5%-73.9, P = 0.77, respectively). The present study was conducted in accordance with the Declaration of Helsinki and was approved by our institutional review board (approval number: 22-095). The dataset was locked on July 31, 2023.

PET-CT imaging procedures

All PET/CT images were acquired using PET/CT scanners (Discovery ST Elite Performance, GE Medical

Systems, Milwaukee, WI, USA [January 2011 to June 2017]; Discovery IQ ODYSSEY 5R, GE Medical Systems, Milwaukee, WI, USA [June 2017 to July 2021]) according to our institution's standardized protocol.[4] Initially, patients were prepared by fasting for at least six hours, discontinuing any anti-diabetic therapies, and ensuring that serum glucose levels remained within 200 mg/dL. Subsequently, patients received an intravenous injection of a standard dose of 4.3 MBq/kg ^{18}FDG (maximum 350 MBq). Between sixty to seventy-five minutes post-FDG injection, a low-dose CT scan (120kV and 150mA) was obtained and combined with a PET scan, imaging from the skull to the midthigh level. The CT acquisition was performed with a tube rotation of 0.5 seconds, section thickness of 3.26 mm, and a pitch of 1.375:1. The matrix and voxel sizes of the acquired images were 128 × 128 and 3.75 × 3.75 × 3.75 mm for Discovery ST Elite Performance and 192 × 192 and 3.26 × 3.26 × 3.26 mm for Discovery IQ ODYSSEY 5R. Once reconstructed, the PET/CT images were evaluated by a well-trained nuclear medicine physician (YM), who was blinded to the clinical data.

Measurement of PET/CT-derived parameters

The standardized uptake value (SUV) was calculated using the following formula: tissue radioactivity concentration (Bq/mL) divided by the injected dose (Bq) per body weight (g). Total metabolic tumour volume (TMTV) was defined as the sum of the volume of visually identified lymphoma lesions with an SUV of ≥ 4 as the absolute threshold.[5] Total lesion glycolysis (TLG) was calculated by multiplying TMTV by mean SUV. For tumour delineation and calculation of radiomic parameters, a semi-automatic computer-aided analysis of PET/CT images was conducted using the open-source software Metavol (Hokkaido University, Sapporo, Japan).[6] The Metavol software automatically highlights all voxels with an SUV≥4.0 from the entire image. We then manually excluded physiological uptakes, including those in the brain, heart, and urinary tract, as well as any apparent inflammatory accumulations. As per a previous proposal,[7] increased ^{18}FDG uptake in the spleen was considered lymphoma involvement only if there were focal areas with ^{18}FDG uptake 1.5 times greater than that in the liver, while bone marrow involvement was included in volume measurements if focal lesions were present, irrespective of the intensity of ^{18}FDG uptake.

Quantification of intratumoural cell populations

Samples obtained from lymph nodes or extranodal lesions were processed immediately after the biopsy. After the mechanical dissociation, the tissues were filtered through a 40-µm nylon mesh and then centrifuged at 500g for 15 minutes at room temperature, after which the supernatant was carefully decanted.[8] The cell pellet was then washed with phosphate-buffered saline. Subsequently, the cells were stained with a panel of antibodies including CD45-KrO, CD19-APC, CD3-FITC, CD4-FITC, CD8-PE, and CD56-

PE (if available). Within the acquired mononuclear cells, the proportions of CD19+, CD3+, CD4+, CD8+, and CD56+ cells were quantified after gating based on the characteristic forward and side scatter patterns and CD45 positivity specific to lymphocytes. While the tissue sampling manner was not strictly limited to an excisional biopsy, a minimum of 10000 mononuclear cells per sample was required, based on a previous study.[9] Data were acquired on a Navios flow cytometer using the Kaluza software (Beckman Coulter, CA, USA).

Statistical analysis

Statistical analyses were performed with R version 4.1.1 (R Foundation, Vienna, Austria). Continuous variables were analysed using the Mann–Whitney U test, while categorical variables were compared using the Fisher's exact test. Pearson correlation analysis was employed to examine the relationships between radiomic features and cellular content within tumours. To maximize predictive power, optimal cut-off values were determined using receiver operating characteristic (ROC) curves for 3-year PFS and 3-year OS. The DeLong's test was used to compare the areas under the curve from two correlated ROCs. The PFS and OS were estimated using the Kaplan–Meier methods and compared with the log-rank test. Univariate and multivariate analyses were conducted using Cox proportional hazards models to assess the factors affecting PFS and OS. Statistical significance was defined as a two-sided P-value of <0.05.

References (supplementary methods)

1. Hans CP, Weisenburger DD, Greiner TC, et al. Confirmation of the molecular classification of diffuse large B-cell lymphoma by immunohistochemistry using a tissue microarray. Blood. 2004;103(1):275-82.

2. Swerdlow SH, Campo E, Pileri SA, et al. The 2016 revision of the World Health Organization classification of lymphoid neoplasms. Blood. 2016;127(20):2375-90.

3. Cheson BD, Fisher RI, Barrington SF, et al. Recommendations for initial evaluation, staging, and response assessment of Hodgkin and non-Hodgkin lymphoma: the Lugano classification. J Clin Oncol. 2014;32(27):3059-68.

4. Terao T, Machida Y, Hirata K, et al. Prognostic Impact of Metabolic Heterogeneity in Patients With Newly Diagnosed Multiple Myeloma Using 18F-FDG PET/CT. Clin Nucl Med. 2021;46(10):790-6.

5. Kurtz DM, Green MR, Bratman SV, et al. Noninvasive monitoring of diffuse large B-cell lymphoma by immunoglobulin high-throughput sequencing. Blood. 2015;125(24):3679-87.

6. Hirata K, Kobayashi K, Wong KP, et al. A semi-automated technique determining the liver standardized uptake value reference for tumor delineation in FDG PET-CT. PLoS One. 2014;9(8):e105682.

7. Barrington SF, Meignan M. Time to Prepare for Risk Adaptation in Lymphoma by Standardizing Measurement of Metabolic Tumor Burden. J Nucl Med. 2019;60(8):1096-102.

8. Witzig TE, Banks PM, Stenson MJ, et al. Rapid immunotyping of B-cell non-Hodgkin's lymphomas by flow cytometry. A comparison with the standard frozen-section method. Am J Clin Pathol. 1990;94(3):280-6.

9. Keane C, Gill D, Vari F, Cross D, Griffiths L, Gandhi M. CD4(+) tumor infiltrating lymphocytes are prognostic and independent of R-IPI in patients with DLBCL receiving R-CHOP chemo-immunotherapy. Am J Hematol. 2013;88(4):273-6.

Supplementary Table 1. Comparison of baseline characteristics between patients with or without sufficient FCM data

	Patients without sufficient FCM data (n=258 [60.1%])	Patients included for analysis (n=171 [39.9%])	P-value
Age, year, median (IQR)	74 (66-80)	71 (61-79)	0.006
Age >60, n (%)	227 (88.0)	130 (76.0)	0.002
Female, n (%)	119 (46.1)	80 (46.7)	0.972
ECOGPS ≧2, n (%)	78 (30.2)	37 (21.4)	0.063
LDH >UNL, n (%)	172 (66.7)	115 (67.8)	0.983
Ann Arbor stage ≧3, n (%)	154 (59.7)	101 (59.1)	0.977
Number of EN lesions ≧2, n (%)	80 (31.0)	38 (22.2)	0.059
IPI, n (%)			
0-2	115 (44.6)	89 (52.0)	-
3-5	143 (55.4)	82 (48.0)	0.156
Disease type, n (%)			
DLBCL, NOS	242 (93.8)	156 (91.2)	0.414
t-FL	12 (4.7)	8 (4.7)	1
EBV-positive DLBCL	4 (1.6)	7 (4.1)	0.187
COO according to Hans algorithm, n (%)			
GCB type	81 (31.4)	48 (28.1)	0.53
non-GCB type	118 (45.7)	89 (52.0)	0.237
Missing	59 (22.9)	34 (19.9)	0.539
PET/CT parameters, median (IQR)			
SUVmax	19.6 (14.4-26.5)	20.8 (14.9-26.9)	0.573
TMTV (mL)	176.2 (51.5-530.2)	177.8 (47-560)	0.961
TLG	1418.3 (384.8-4637.5)	1683.4 (352-5557.4)	0.832

Biopsied lesion, n (%)			
LN	117 (45.3)	144 (84.2)	<0.001
EN lesion	141 (54.7)	27 (15.8)	<0.001
GI tracts	58 (22.5)	3 (1.8)	<0.001
BM	14 (5.4)	0 (0)	0.005
Other lesions	69 (26.7)	24 (14.0)	0.003
Induction regimen, n (%)			
R-CHOP	220 (85.3)	149 (87.1)	0.687
More intensive chemotherapy	20 (7.8)	13 (7.6)	1
Less intensive chemotherapy	18 (7.0)	9 (5.3)	0.608
CR achievement at end of induction, n (%)	193 (74.8)	139 (81.3)	0.146

Abbreviations: TI, tumour-infiltrating; IQR, interquartile range; ECOGPS, European Cooperative Oncology Group Performance Status; LDH, lactate dehydrogenase; UNL, upper normal limit; EN, extranodal; IPI, International Prognostic Index; DLBCL, NOS, diffuse large B-cell lymphoma, not otherwise specified; t-FL, DLBCL transformed from follicular lymphoma; EBV, Epstein-Barr virus; COO, cell of origin; GCB, germinal center B-cell; SUV, standard uptake value; TMTV, total metabolic tumour volume; TLG, total lesion glycolysis; LN, lymph node; EN, extranodal; GI, gastrointestinal; BM, bone marrow; R-CHOP, rituximab combined with cyclophosphamide, doxorubicin, vincristine, and prednisone; CR, complete remission.

Supplementary Figure 1. Flow diagram of patient enrolment for analysis.

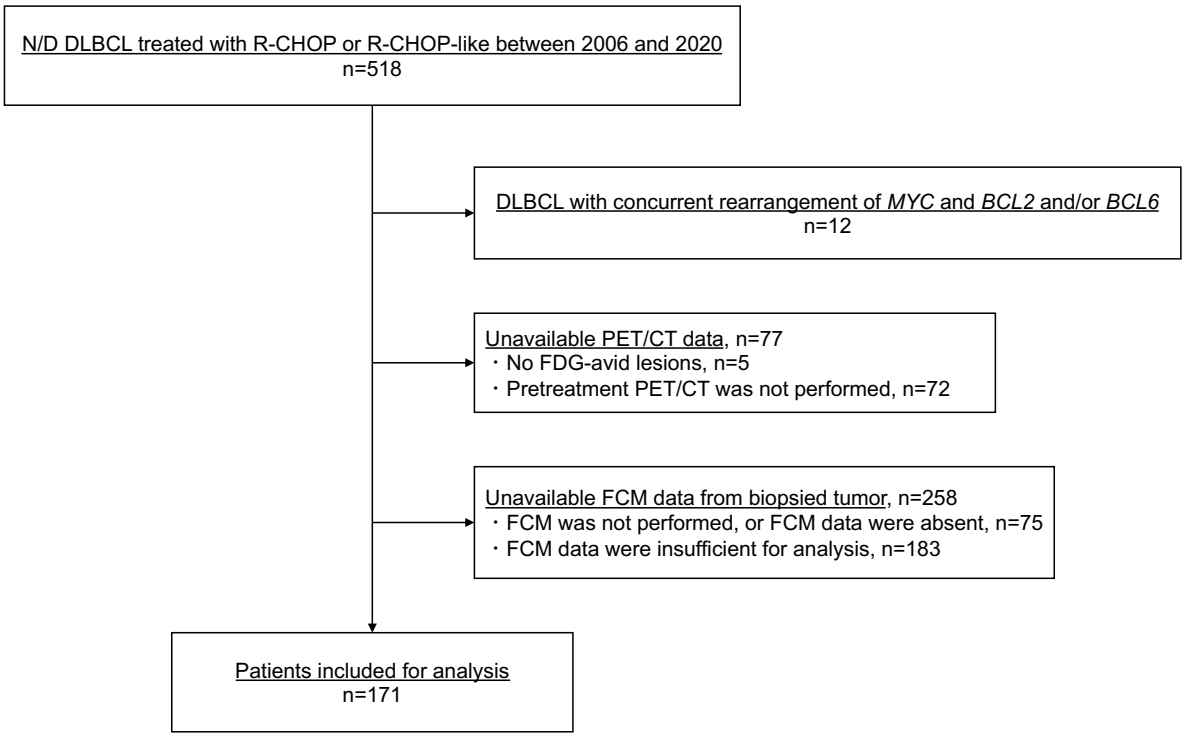

Abbreviations: N/D, newly diagnosed; DLBCL, diffuse large B-cell lymphoma; FDG, Fluorine-18 fluorodeoxyglucose; PET/CT, positron emission tomography/computed tomography; FCM, flow cytometry.

Supplementary Figure 2. ROC analysis to determine optimal cut-offs for predicting 3-year PFS and OS.

A) ROC for intratumoural lymphocyte subsets and B) ROC for radiomic parameters.

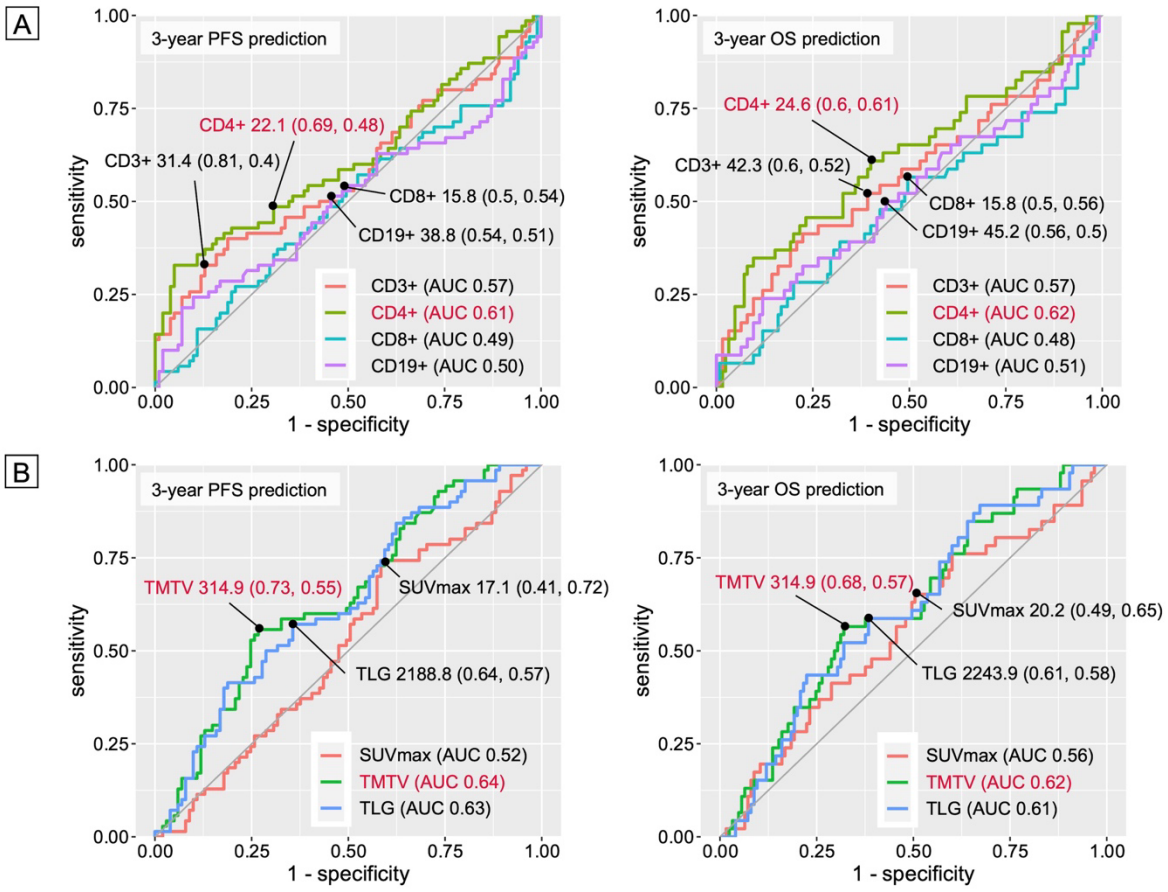

Abbreviations: PFS, progression-free survival; OS, overall survival; AUC, area under the curve; TMTV, total metabolic tumour volume; TLG, total lesion glycolysis.

Supplementary Figure 3. Comparison of tumour-infiltrating cell proportions between EBV-positive and EBV-negative DLBCL patients. A) CD19+ cells, B) CD3+ cells, C) CD4+ cells, and D) CD8+ cells.

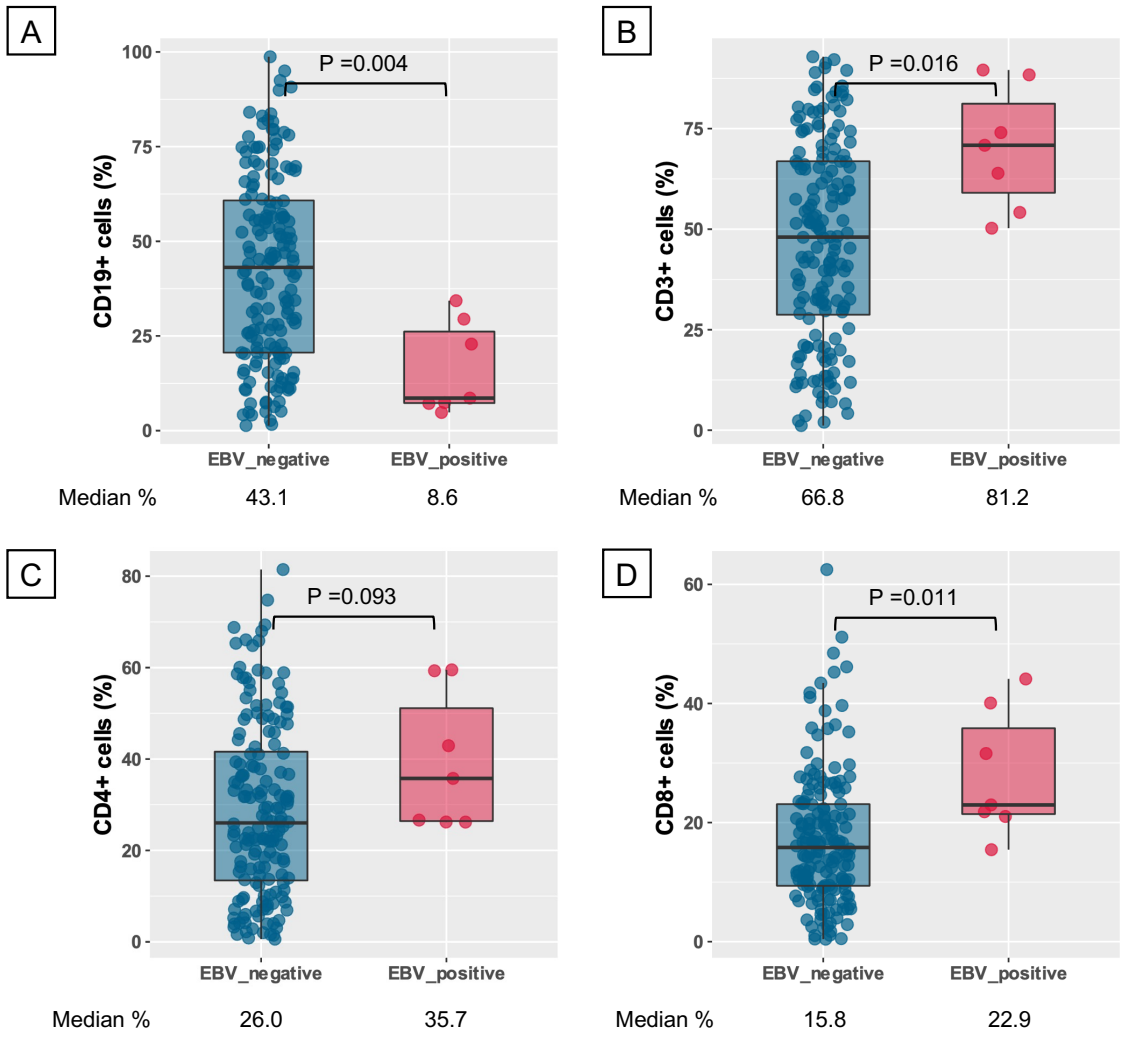

Abbreviations: EBV, Epstein-Barr virus; DLBCL, diffuse large B-cell lymphoma.

Supplementary Figure 4. Prognostic relevance of tumour-infiltrating CD4+ cells in biopsied extranodal lesions. A) Pie chart showing the distribution of biopsied organs. B) Comparison of intratumoural lymphocyte proportions between lymph nodes and extranodal lesions. C) Kaplan-Meier estimates of OS and D) PFS based on the CD4+ cell burden within extranodal lesions.

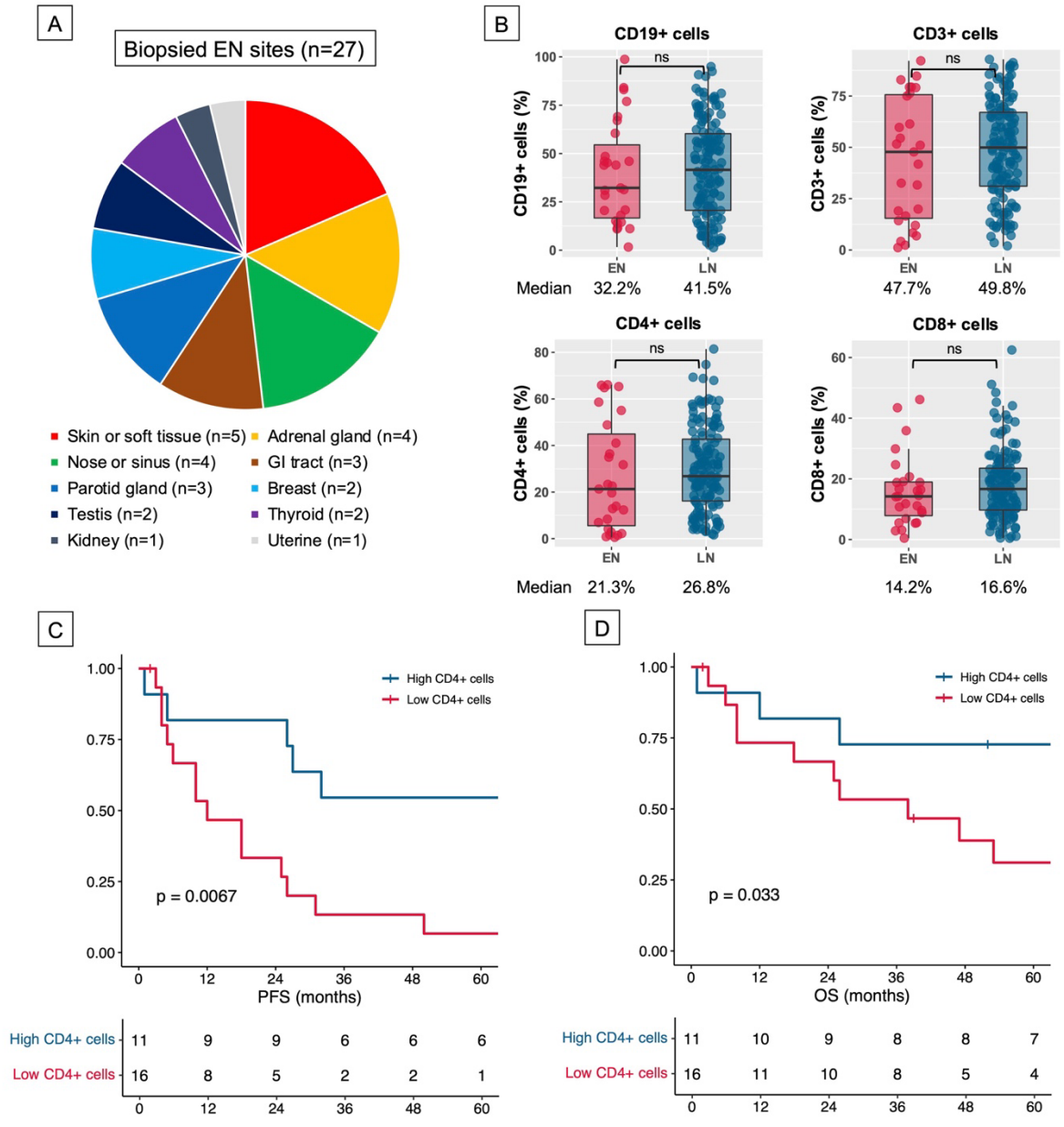

Abbreviations: EN, extranodal; PFS, progression-free survival; OS, overall survival.